Heliyon 10 (2024) e30823

Contents lists available at ScienceDirect

Heliyon

journal homepage: www.cell.com/heliyon

Research article

Optimization use of watermelon rind in the coagulation-flocculation process by Box Behnken design for copper, zinc, and turbidity removal

Salma Kouniba, Asmaa Benbiyi *, Ali Zourif, Mohamed EL Guendouzi

Laboratory of Physical Chemistry, Material & Catalysis LCPMC, Faculty of Sciences Ben M'Sick, University of Hassan II-Casablanca, Morocco

A R T I C L E I N F O

Keywords:
Watermelon rind
Coagulation-flocculation
Metals
Turbidity
Response surface method
Box Behnken design

A B S T R A C T

Watermelon rinds were investigated as a bio-coagulant for treating water contaminated by metals and turbidity, owing to their biodegradability and greater environmental friendliness compared to chemical coagulants. Fourier transform infrared spectroscopy, scanning electron microscopy paired with energy dispersive X-ray analysis and X-ray diffraction characterized the watermelon rinds before and after use. A Box-Behnken experimental design optimized the most influential parameters of initial pH, coagulant dose, and particle size based on response surface methodology. This analysis revealed the experimental data fit quadratic polynomial models, achieving maximum removal efficiencies of 97.51 % for zinc, 99.88 % for copper, and 99.21 % for turbidity under optimal conditions. Statistical analysis confirmed the models effectively captured the experimental data. Analysis of variance denoted the high significance of the quadratic effects of dose and pH. Removal of metal ions Zn^{2+} and Cu^{2+} was significantly impacted by these factors. The watermelon rind powder retained its coagulation efficiency after five cycles of reuse, with removal rates of 80.04 % for Zn, 88.33 % for Cu and 86.24 % for turbidity. These results demonstrate the potential of watermelon rind as an alternative coagulant for wastewater treatment. Further testing on real industrial effluents at larger scales would help assess their feasibility for real-world applications.

1. Introduction

Several industries discharge a variety of wastes into the environment, including mineral and organic pollutants such as concentrated detergents, aromatic compounds, metals and dyes. These have adverse effects on human health, economic productivity, the quality of environmental freshwater resources, and ecosystems [1]. Metallic pollution is considered the most dangerous and harmful, as it is non-degradable, toxic and carcinogenic [2]. The progressive and continuous accumulation of metals in water and soil can cause toxicity in many living organisms and pollution in aquatic environments and agricultural soils [3]. In recent years, there has been a worldwide increase in the annual production of copper (Cu) and zinc (Zn), compared to other metals such as Pb, Cd, Cr, Ni, As and Hg [4]. However, Cu and Zn are essential elements, vital in small quantities for various physiological functions. Cu is involved in energy production and antioxidant defenses, while Zn plays crucial roles in DNA synthesis, immune function, and wound healing. Both are indispensable for overall health, but their balanced intake is crucial as deficiencies and excess can lead to health issues [5]. Several

* Corresponding author.
E-mail addresses: a.benbiyi@gmail.com, asmaa.benbiyi@etu.univh2c.ma (A. Benbiyi).

https://doi.org/10.1016/j.heliyon.2024.e30823
Received 23 September 2023; Received in revised form 20 April 2024; Accepted 6 May 2024
Available online 8 May 2024
2405-8440/

studies deduced that accumulation of Cu and Zn in the organism can cause physiological disorders, complications in the respiratory system and skin diseases [6], neurological disorders, such as Alzheimer and depression [7,8]. More, in aquatic environment, aquatic species like fish, invertebrates and algae are generally more sensitive to Cu and Zn in water because of their toxicity even at lower concentrations [9,10].

Alternative treatment techniques have become a necessity for our environment. Indeed, various methods have been used to remove metals from industrial wastewater, including electrochemical and biological treatments [11,12], oxidation [13], adsorption [14] and coagulation-flocculation [15]. The latter process was chosen for metal pollution removal because of its simplicity, rapidity of treatment, high efficiency, easy separation of treated water and adsorbed pollutants, as well as the availability of coagulants and flocculants [16,17].

Sustainable plant-based green coagulants have replaced chemical because of their effectiveness, biodegradability and greater respect for the environment. Studies have reported that plant waste and fruit peels used as coagulants have shown good effectiveness in removing various pollutants from wastewater [18,19]. In fact, Moringa Oleifera seeds exhibited 99.8 % turbidity (TUR) removal efficiency, owing to their protein-rich compositions that act as cationic polyelectrolytes in the coagulation/flocculation process [20]. The coagulation potential of Moringa gland, cotyledons and husk as sources of active components have been used for TUR removal [21]. Studies on natural coagulants chitosan and Moringa oleifera have shown their great capacity as a coagulant with an efficiency of approximately 95.35 % and 94.8 % for water of medium TUR (314.4 NTU) [22]. Plant mucilage, a viscous polysaccharide-rich extract from fruits or plants such as “dragon fruit”, can remove up to 70 % TUR, 60 % COD, and 90 % color from various wastewaters [23]. Fruit peels are, non-edible, and renewable polymeric materials that are discarded as waste [24]. Banana peel as a coagulant exhibited 90 % TUR elimination from synthetic wastewater [25], and has been utilized as a bio-adsorbent for removing soluble contaminants including dyes [26] and metals [27].

For that we have choose to study the effectiveness of fruit peels like watermelon rind (WMR) as a bio-coagulant for the removal of metals and turbidity by the coagulation-flocculation process. In fact, WMR is abandoning, presenting a high adsorption capacity for metals and little studied as a coagulant [28]. Watermelon *“Citrullus lanatus”* is a globally cultivated fruit known for its high water content, and low calorie count [29]. In Morocco, the whole area used for the cultivation of watermelon in 2018 was around 17,600 ha, with an average density of 3000 plants/hectare. Average national production is estimated at 40 t/ha, exceeding 60 t/ha in Gharb, 37 % in Marrakech-Tensift-Al Haouz, and 19 % in Souss Massa regions [30]. However, despite the occasional use of WMR in vinegar, or as a cooked vegetable [31], these valuable resources are often thrown away, resulting in substantial quantities of wasted seeds and rinds. WMR has surfaced as a viable and sustainable adsorbent, showcasing promise in the removal of metals such as Cd and Zn from aqueous solutions. It demonstrates notable adsorption capacities, with values of 31.35 mg/g for Cd [32] and 25 mg/g for Zn [33]. Additionally, activated watermelon shell based biosorbent exhibit high efficiency in the removal of Cu and Zn, achieving rates of 88 % and 90.3 %, respectively [34].

Indeed, it’s important to highlight the under-explored potential of WMR as a bio-coagulant, given the scant attention it receives in the existing literature. The limited number of studies focusing on its coagulation properties highlights a research gap that our work aims to fill. Using experimental designs as an optimization tool, we aimed to improve the effectiveness of WMR, recognizing the need for systematic exploration and improvement. An experimental design offers advantages, including the ability to refine process parameters, minimize experimental deviations and accurately determine optimal conditions. The effects and interactions of various parameters on removing pollutants from contaminated waters were determined using the response surface methodology (RSM), based on the Box-Behnken design (BBD) [35]. Three independent parameters were selected, such as coagulant dose, granulation, and initial pH of the solution. These parameters were examined to optimize pollutant removal efficiency while minimizing the required number of experimental trials, energy and cost.

Various techniques like, Fourier transform infrared spectroscopy (FTIR), scanning electron microscopy paired with energy dispersive X-ray analysis (SEM-EDX) and X-ray diffraction (XRD) were used to characterize the WMR before and after use, in order to deduce and understand the underlying mechanisms and to identify the specific interactions during the coagulation flocculation process. The reuse of bio-coagulant has also been tested for several cycles to ensure a sustainable coagulation-flocculation process in wastewater treatment.

2. Materials and methods

2.1. Preparation of coagulant

Watermelon fruit were obtained from a local market. The rinds were washed with distilled water to eliminate all impurities. After washing, the rinds were oven-dried at 105 °C for 24 h, then ground and sieved to achieve powders with diameters of 60, 90, and 120

Table 1
Sample information.

Compound	CAS No	Source	Initial mass fraction purity given by suppliers	Molecular weight (g. mol^{-1})
$ZnSO_4 \cdot 7H_2O$	7446-20-0	Sigma-Aldrich	99 %	287.560
$CuSO_4 \cdot 5H_2O$	7758-99-8	FLUKA	98 %	249.690
HCl	7647-01-0	Sigma-Aldrich	37 %	36.458
NaOH	1310-73-2	Sigma-Aldrich	99 %	39.997

µm for use as a bio-coagulant [28]. The WMR obtained was directly utilized for the coagulation tests without chemical treatment.

2.2. Preparation of the pseudo samples of water

A variety of products were used in the pseudo-sample preparation process. Table 1 summarizes the product information. Pseudo samples were prepared with initial concentrations of 50 mg. L^{-1} for Cu and 20 mg. L^{-1} for Zn, representing 100-fold typical limits for direct aquatic discharge of metals in Morocco [36]. To produce turbid water, a 10 g. L^{-1} kaolin suspension was prepared by dispersing kaolin in water with 1-h stirring for uniformity. After resting for 24 h to fully hydrate particles [37], this stock suspension served as the basis for preparing water samples with varying turbidity levels for bio-coagulation assays.

2.3. Coagulation-flocculation experiments

The different coagulation-flocculation tests are performed using the Jar-Test consisting of a series of 4 jars (VELP Scientifica JLT 4 Flocculator). This instrument allows the simultaneous agitation of the solutions with a speed of rotation that reaches 300 rpm. The solution is mixed quickly at 300 rpm for 2 min, followed by a slow agitation of 60 rpm for 20 min, then a decantation for 1 h and finally a filtration. The final concentrations of Cu and Zn in the samples are determined using inductively coupled plasma mass spectrometry (ICP-MS Ultima Expert). The calculation of abatement is necessary to know the rate of elimination of metals; it is calculated by Eq. (1).

$$\text{Abatement\%} = \frac{C_i - C_f}{C_i} \times 100 \tag{1}$$

with, C_i and C_f are the initial and final concentration of the metal.

TUR is measured with a VELP SCIENTIFICA Turbidimeter with a range from 0 to 1000 NTU (Nephelometric Turbidity Units). The turbidity removal rate (TRR) is defined by Eq. (2).

$$(\text{TRR})\% = \frac{\text{Initial Turbidity} - \text{Final Turbidity}}{\text{Initial Turbidity}} \times 100 \tag{2}$$

2.4. The point of zero charge (PZC)

The point of zero charge (PZC) was experimentally determined by assessing surface charge at various pH values to identify the neutral point using potentiometric titration [38]. A quantity of 0.01 g of WMR was evenly distributed among several 100 mL beakers containing 50 mL of an electrolytic medium with a KNO_3 concentration of 0.03 M. The initial pH_i values of these beakers ranged from 2 to 10.

2.5. Characterization techniques

WMR were characterized by X-ray diffraction (XRD) to undertake the mineralogy, Fourier transform infrared spectroscopy (FTIR) for identifying functional groups, and scanning electron microscopy (SEM) coupled with energy dispersive Xray analysis (EDX) to determine the morphology and the elemental composition of WMR. Xray diffraction patterns were obtained using a diffractometer (Xpert Datacollecter) with CuKα radiation ($\lambda = 1.5418$ Å). FTIR spectra were acquired from a Bruker Tensor 27 spectrometer operating in the 4000 - 400 cm^{-1} range. SEM imaging (Hirox SH-4000 M) coupled with EDX spectroscopy (Bruker) provided microstructural and elemental analysis of the WMR. Additionally, the coagulation-flocculation sludge underwent characterization by FTIR, XRD and SEM-EDX in order to deduce and understand the mechanism of coagulation-flocculation process.

2.6. Box-Behnken design (BBD)

The Box-Behnken method is a statistical tool for the experimental design, calculating the interaction effects between various factors and determining the optimum conditions for the desired outcomes.

A BBD employing three-level continuous factors was utilized, with interpretation based on second-order models, for the examination of three factors (coagulant dose, granulation and initial solution pH), and three response variables (Zn, Cu, and TUR removal rates). Factor coding and range selection normalized the chosen parameters to improve model equation accuracy [39]. Since examining all influential factors was impractical for economic reasons, the selection focused on those with major effects. Indeed, in the coagulation-flocculation process, the three factors mentioned above were identified as the most significant and influential factors.

Optimizing dose becomes especially important for charge neutralization mechanisms [40]. The granulation and size distribution of coagulants have a significant influence on the mechanism of the coagulation-flocculation process. Studies by Sun et al. showed increasing particle numbers noticeably affects system physical properties [41]. As numbers rise, sizes decrease, heightening Brownian motion. This enhances particle collisions, producing denser floc morphologies. Undoubtedly, solution pH is a vital parameter controlling coagulation-flocculation, substantially impacting particle surface charge and coagulant behaviors [42].

The number of experiments (N) required for a three-factor BBD is given by Eq. (3): [43] **[43]**

$$N = 2(k\ (k\text{-}1)) + n_0 \tag{3}$$

The BBD for three factors composed of 15 tests.

With, n_0: the number of central points, and k: the number of factors.

To that effect, the BBD adopted for the three factors will subsequently require the planning of 15 experimental tests. The mathematical model associated with this matrix is given by Eq. (4) [43].

$$Y = a_0 + \sum_{i=1}^{k} a_i X_i + \sum_{i=1}^{k} a_{ii} X_i^2 + \sum_{i=1}^{k} 1 \sum_{j=1}^{k} a_{ij} X_i X_j + \varepsilon \tag{4}$$

With, Y: the experimental response (the elimination rate),

a_0: a constant,

a_i: the main effect of factor i,

a_{ii}: the quadratic effect (squared),

a_{ij}: the interaction effect between factors i and j,

ε: is the random error between the predicted and measured values.

3. Results and discussion

3.1. Characterization of the WMR

3.1.1. Structural analysis XRD

The WMR X-ray diffractogram exhibits a broad diffraction background without sharp peaks, indicating a predominantly amorphous structure typical for organic materials (Fig. 1a).

Two observable peaks at 2θ = 24° and 42° correspond to crystalline carbon, with expanded lattice parameters due to carbon impurities. The presence of crystalline peaks is attributed to the cellulosic fraction within the WMR [44]. No change is observed on WMR in the diffractograms after the coagulation-flocculation process (Fig. 1b and c).

3.1.2. FTIR spectra

The FTIR spectrum of WMR in Fig. 2a exhibits several peaks corresponding to different functional groups. Frequencies from 3883 to 3834 cm^{-1} signify –OH stretching, potentially due to pellets and KBr used in sample preparation. A peak around 3430 cm^{-1} indicates NH and OH stretching vibrations, with broadening suggesting hydrogen bonding to solvent. An intense broad peak at approximately 3468 cm^{-1} arises from –OH vibrations of cellulose and lignin. The 2920 cm^{-1} peak corresponds to aliphatic CH stretching. At 1734 cm^{-1}, a peak represents C=O stretching of carboxylic acids or esters. Another peak around 1634 cm^{-1} relates to carboxylic acid C=O stretching. Furthermore, the 1380 cm^{-1} peak is attributed to symmetric –COO– stretching of pectin groups [28]. FTIR analysis demonstrates WMR contains various functional groups like NH, COOH, C=O, and –COO–, which could serve as potential adsorption sites for metal ions. After coagulation-flocculation treatment (Fig. 2b and c), the 3430 cm^{-1} stretching band shifted to 3421 cm^{-1} and broadened. The 1634 cm^{-1} peak shifted to 1628 cm^{-1}. The 1380 cm^{-1} peak disappeared, while the 2920 cm^{-1} peak enlarged. These shifts potentially correspond to functional group energy changes, suggesting carboxyl and hydroxyl groups predominantly contribute to metal removal through complexation [45].

3.1.3. SEM -EDX analysis

SEM images in Fig. 3a reveal WMR has a porous texture with considerable rough heterogeneous pore layers, providing ample

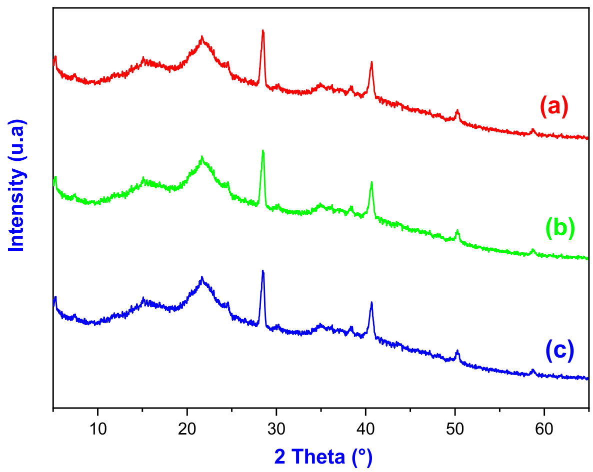

Fig. 1. XRD diffractograms: (a) raw powder of WMR; (b) Cu and (c) Zn sludges after coagulation treatment.

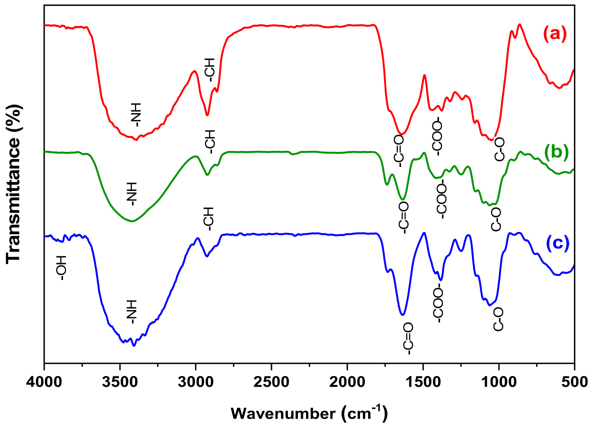

Fig. 2. FTIR spectra: (a) raw powder of WMR; (b) Cu and (c) Zn sludges after coagulation treatment.

surface area for pollutants adsorption. An increase in WMR particle size was observed by SEM after coagulation-flocculation process (Fig. 3b and c), confirming the binding of pollutants to the WMR surface. The SEM contains secondary and backscattered electron detectors for imaging alongside an energy dispersive X-ray (EDX) analyzer. EDX analysis of WMR before coagulation showed that it is composed of 57.53 % C, 25.50 % O, 8.96 % K, 1.19 % Cl, 1.27 % Al, 1.16 % P, 0.76 % S, 0.48 % Ca, 2.03 % Fe, 0.11 % Mg and traces of Cu and Zn (Table 2). The chemical composition determined by EDX shows that WMR is predominantly composed of carbon and oxygen, with significant proportions of the above elements and low levels of Cu and Zn. However, Cu and Zn concentrations reach around 6 % in the sludge after treatment by coagulation-flocculation. These chemical and structural characteristics confirm the porous and heterogeneous texture of WMR, with a large specific surface area, making it a good adsorbent for metal ions, and make from WMR a promising material for coagulation-flocculation applications.

3.1.4. The determination of PZC

The point of zero charge (PZC) indicates the pH where a solid's surface charge reaches neutrality. Below the PZC, the surface has a positive charge, while above, it becomes negatively charged. Fig. 4 illustrates the plot of the difference between initial and final pH values (ΔpH) against the initial pH (pHi). While the PZC is crucial as it allows predicting the electrostatic interactions between WMR and metal ions in solution. Through experimental determination, the PZC for WMR was established at 7.6. At pH levels below 7.6, the WMR surface undergoes protonation, resulting in a positive charge. Conversely, when the pH exceeds 7.6, the surface becomes negatively charged. This pH dependent charge variation on the WMR surface predicts a preference for the adsorption of Zn^{2+} and Cu^{2+} ions at pH levels above 7.6, facilitated by electrostatic attraction between the negatively charged surface and the metal ions. This underscores the significance of pH as a determining factor in the coagulation-flocculation process of Zn^{2+} and Cu^{2+} by WMR.

3.2. Modeling by the Box-Behnken method

The Box-Behnken method is a statistical experimental design technique used for modeling and optimizing processes. It is particularly useful to study the effects of multiple factors on a response variable while minimizing the number of experimental runs. This method is commonly used in industries such as chemistry, engineering, and manufacturing. In the coagulation-flocculation process, critical factors were assigned codes. X_1 denotes coagulant dose, X_2 is particle size, and X_3 is initial solution pH. Table 3 presents the experimental matrix code for the BBD. The JMP software "John's Macintosh Project" was used to generate the experimental matrix, estimate the effects, and analyze the results. Table 4 shows the experimental results (Y_1, Y_2, Y_3) alongside estimated values (Y'_1, Y'_2, Y'_3) from the BBD, where Y is the experimental removal rate and Y′ is the estimated rate.

3.2.1. Analysis of variance (ANOVA)

ANOVA was utilized to assess the statistical significance of the quadratic regression model and its individual terms. The P-value and F-value were employed as measures to analyze the variable, interaction, and quadratic effect impacts [46]. Table 5 presents ANOVA results for the quadratic response surface models.

The considerable F-values indicate the regression equations effectively model the predicted response variations. The associated probability value (P) determines whether the F-value is statistically significant, with $P < 0.05$ denoting at least one regression term is significantly correlated to the dependent variable [43]. Based on the ANOVA results for Zn, Cu, and TUR removal percentages, the models are significant, with respective F-values of 82.90, 10.16, and 7.94. The calculated R^2 values of 0.9981, 0.9581, and 0.9546 signify the independent variables explain over 90 % of response variance at a 95 % confidence level [47].

Quadratic polynomial models determined the relationships between coagulation capacity and dose, size and pH. The elimination model equations for Zn (Y_1; Eq. (5)), Cu (Y_2; Eq. (6)) and TUR (Y_3; Eq. (7)) are as follows:

$$Y_1 = 32.04 + 0.12X_1 + 8.9X_3 + 0.003X_1^2 - 0.32X_3^2 - 0.03X_1X_3 \quad (5)$$

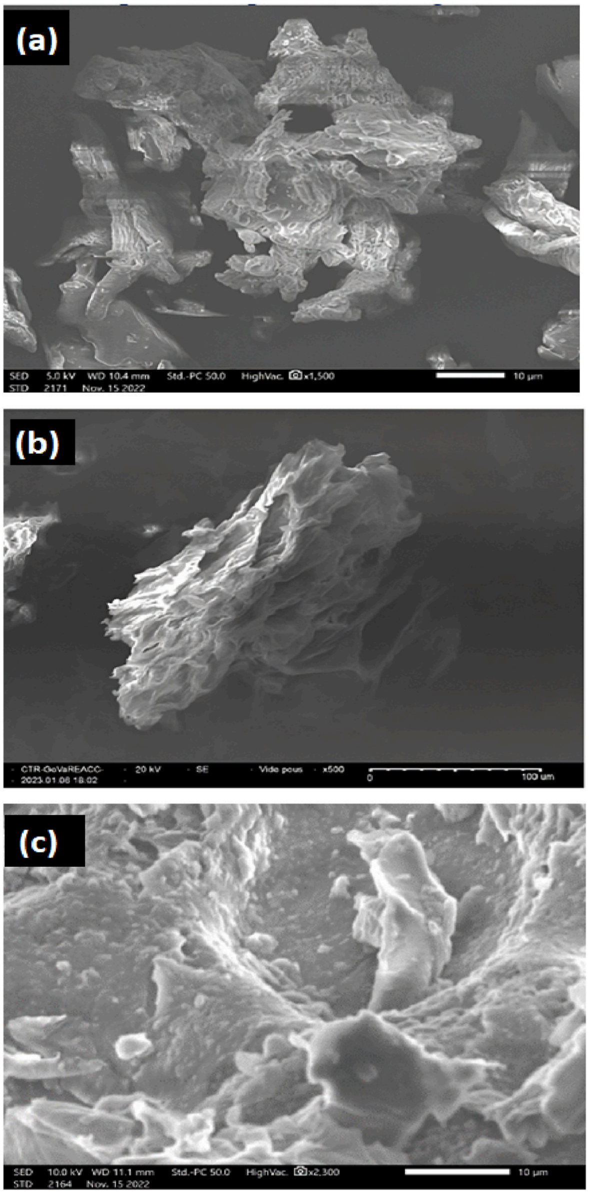

Fig. 3. SEM micrographs: (a) raw powder of WMR; (b) Cu and (c) Zn sludges after coagulation treatment.

Table 2
Chemical composition (EDX) of WMR before and after coagulation-flocculation.

Element %	C	O	K	Cl	S	Ca	Al	P	Fe	Mg	Cu	Zn
Raw powder of WMR	57.53	25.5	8.96	1.27	0.76	0.48	1.27	1.16	2.03	0.11	0.04	0.02
Zn sludge	59.40	27.01	4.32	0.67	0.42	0.29	0.76	0.83	1.03	0.10	0.04	5.98
Cu sludge	60.10	27.64	3.26	0.58	0.38	0.19	0.56	0.62	0.54	0.10	6.23	0.02

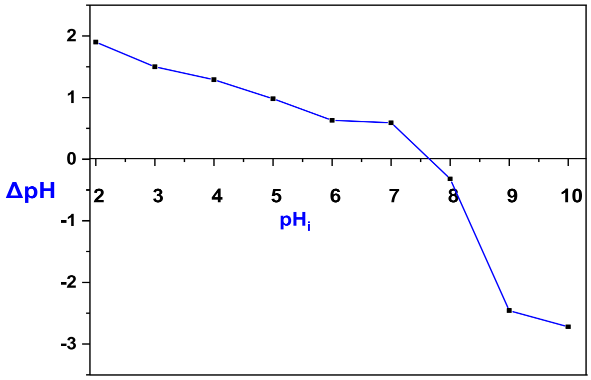

Fig. 4. The Point of Zero Charge plot of WMR.

Table 3
Box-Behnken design matrix.

Factors	Variables	Range and levels		
		−1	0	+1
Dose (mg/l)	X_1	200	350	500
Granulation (µm)	X_2	60	90	120
pH	X_3	3	6	9

Table 4
Experimental and predicted values for Zn, Cu and TUR removal (Y_1, Y_2, and Y_3).

	Factors			Experimental values			Predicted values		
	X_1	X_2	X_3	$Y_{1\ WMR-Zn}$	$Y_{2\ WMR-Cu}$	$Y_{3\ WMR-TUR}$	$Y'_{1\ WMR-Zn}$	$Y'_{2\ WMR-Cu}$	$Y'_{3\ WMR-TUR}$
1	200	60	6	87.73	85.99	98.34	87.301	82.905	98.465
2	200	120	6	87.53	83.62	98.89	87.514	78.165	99.112
3	500	60	6	87.52	88.92	98.02	87.536	94.375	97.797
4	500	120	6	83.28	87.04	97.91	83.709	90.125	97.785
5	350	60	3	73.29	45.57	96.58	73.172	49.317	96.794
6	350	60	9	96.60	98.21	98.24	97.130	92.092	98.124
7	350	120	3	73.92	32.10	97.37	73.390	38.217	97.486
8	350	120	9	93.18	97.95	98.28	93.297	94.202	98.066
9	200	90	3	72.15	37.50	97.88	72.696	36.837	97.541
10	500	90	3	72.62	79.27	96.92	72.721	70.067	96.929
11	250	90	9	96.54	98.53	98.87	96.439	107.732	98.881
12	500	90	9	96.39	97.27	97.16	92.844	97.932	97.499
13	350	90	6	88.78	84.02	98.64	88.497	84.230	98.643
14	350	90	6	88.53	84.81	98.60	88.497	84.230	98.643
15	350	90	6	88.18	83.86	98.69	88.497	84.230	98.643

$$Y_2 = 37 + 0.14X_1 + 15.9X_3 - 1.34X_3^2 - 0.24X_1X_3 \quad (6)$$

$$Y_3 = 93.8 + 1.75X_3 - 0.1X_3^2 \quad (7)$$

Fig. 5a–b and c depicts the relationship between experimental Zn, Cu, and TUR removal by WMR and values predicted by the fitted regression models. The clustering of points around the regression line indicates favorable correlation between experimental and predicted responses, with R^2 exceeding 0.95 signifying robust dependence. However, no combined effects of input variables were observed in the generated response models. Although some interactions were present, their impact on the response was insignificant. The polynomial model goodness-of-fit was assessed using the coefficient of determination (R^2) and adjusted R^2 [48].

3.2.2. The interactive effects of variables on yield

Response surfaces graphically represent the relationship between the response variable and experimental levels of one or more independent variables. Response surfaces visually depict how the response variable relates to the experimental levels of one or more independent variables. In Fig. 6, three-dimensional (3D) response surface plots illustrate the removal of Zn (Fig. 6a), Cu (Fig. 6b), and TUR (Fig. 6c). These plots are generated by maintaining one variable at its optimal level while adjusting the others within defined

Table 5
Results of ANOVA analysis for quadratic model.

	WMR-Zn		WMR-Cu		WMR-TUR	
	F-value	P-value	F-value	P-value	F-value	P-value
Model	82.9036	0.0001[a]	10.1670	0.0100[a]	7.9420	0.0172[a]
X_1	1.0440	0.0904	0.9770	0.1054	0.3370	0.4605
X_2	0.8530	0.1401	0.3160	0.4829	0.6820	0.2079
X_3	3.4570	0.0000[a]	3.3870	0.0004[a]	2.1320	0.0973
X_1X_2	0.7110	0.1945	0.0100	0.9778	0.4730	0.3366
X_1X_3	2.4160	0.0038[a]	1.2970	0.0504	0.5680	0.2701
X_2X_3	0.7100	0.1949	0.3310	0.4669	0.5510	0.2813
X_1^2	3.6150	0.0002[a]	0.6320	0.2330	0.0890	0.8148
X_2^2	3.0000	0.0010[a]	0.3680	0.4285	0.6490	0.2241
X_3^2	3.4570	0.0003[a]	1.3940	0.0403[a]	2.3720	0.0042[a]
Lack of fit	26.0638	0.0372[a]	453.2000	0.0020[a]	78.4139	0.0126[a]
R^2	0.9981	–	0.9581	–	0.9546	–
Adjusted R^2	0.9947	–	0.8549	–	0.8169	–

[a] Significant.

conditions.

The elliptical shape observed in the 3D surface curves signifies a robust and beneficial interaction between the two variables X_1 and X_3. These curves provide an accurate geometric representation and give the appropriate statistics, including the optimal range for different values of the test variables within the experimental design [39].

Initial pH was identified as highly influential, significantly reducing Zn, Cu and TUR levels. WMR showed maximum Zn removal at a value of 96.6 % at basic pH 9 and dose 350 mg. L^{-1}.

The combined dose and initial pH effect on Zn removal are very significant, with removal increasing with dose but decreasing with rising initial pH (Fig. 7). This indicates higher removal is achieved by simultaneously elevating dose and maintaining initial pH 7–9, due to decreasing solution charge density with initial pH [49].

WMR showed maximum Cu removal at a value of 98.53 % under conditions of a basic initial pH 9 and a dose of 250 mg. L^{-1}, whereas the change for granulation was not significant with the same pH and dose conditions. Higher removal occurred by concurrently lowering dose and maintaining initial pH 5–7 (Fig. 8).

WMR showed maximum TUR removal at a value of 98.89 % at approximately neutral pH 6 with a 200 mg coagulant dose. The graph in Fig. 9 illustrate how the relative interaction between pH and coagulant dose impacts turbidity removal performance. After coagulation-flocculation and settling, precipitated and suspended materials can be effectively removed by gravity, generating a clear supernatant with substantially reduced TUR [50].

3.2.3. Optimum conditions using BBD

Optimum conditions are typically determined through rigorous experimentation and data analysis. Table 6 summarizes the experimental and predicted results of Zn, Cu and TUR removal applying the optimum conditions found by the BBD.

3.3. Mechanism of coagulation by WMR

The structural and chemical characterization of WMR before and after treatment of the polluted water, has enabled us to draw a number of important conclusions. WMR is an organic and cellulosic material containing various functional groups like NH, COOH, C=O and –COO–, in addition to K, Al, Fe and other elements. Post-coagulation treatment, a distinct reduction in K, Fe, and Al levels and an elevation in Cu and Zn in the sludge were evident, emphasizing their pivotal role in effectively removing these metals. Ion exchange mechanisms between K, Fe, and Al with Cu^{2+} and Zn^{2+} ions indicate their adsorption onto the WMR surface, releasing their ions into the sludge. Notably, multivalent cations, particularly Fe^{3+} and Al^{3+}, serve as effective coagulant adjuvants, playing a crucial role in charge neutralization and bridging mechanisms during the coagulation process [51].

Natural plant-based coagulants can operate through polymer bridging or charge neutralization [18]. In water, colloids are typically negatively charged. Charge neutralization uses ionizable polymer coagulants to stabilize particles (Fig. 10). Thus, WMR characterization before and after coagulation-flocculation suggests Zn, Cu, and TUR removal occurred via adsorption followed by charge neutralization. Many factors can influence these mechanisms, including hydrogen bonding and van der Waals forces [52]. The adsorption mechanism of these ions is proposed to involve electrostatic attraction between positive Cu^{2+} and Zn^{2+} and negative –COO– and –OH– charges on the WMR surface. This is completed by hydroxyl/carboxyl deprotonation and subsequent metal chelation [53].

3.4. Comparison with previous works

Table 7 provides a comprehensive overview of prior investigations into the elimination of Zn, Cu, and TUR using coagulation-flocculation technique. Diverse biomasses have been tested as bio-coagulants for these contaminants. Furthermore, it is noteworthy

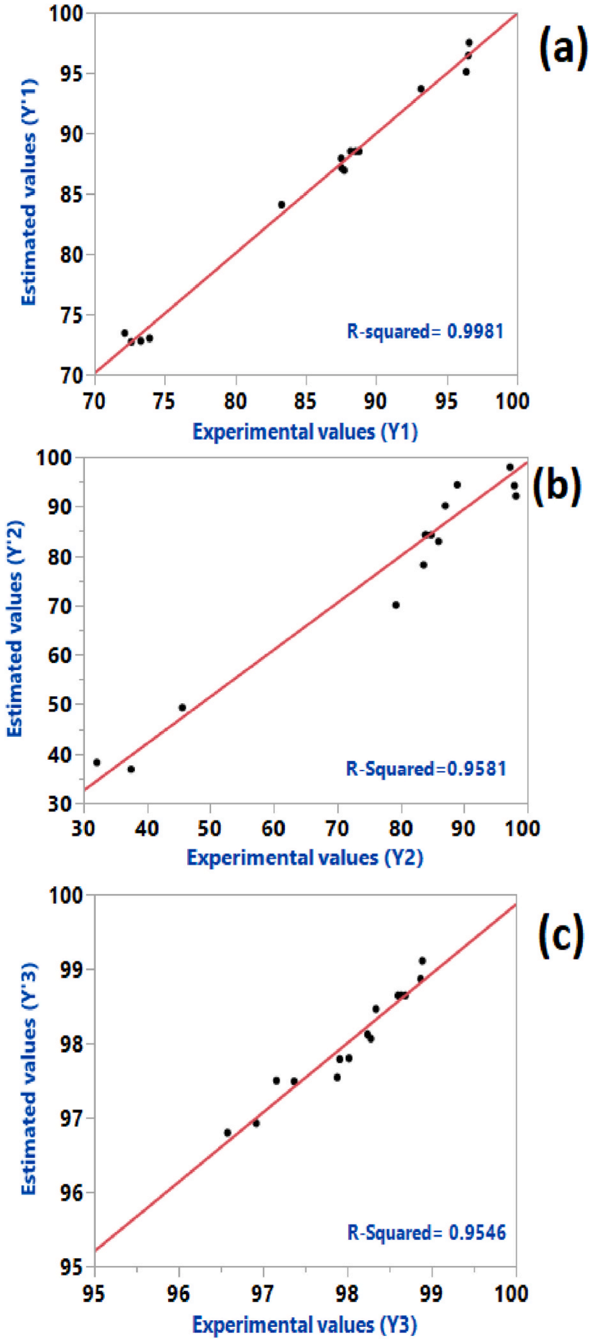

Fig. 5. Experimental values (%) plotted against predicted values (%); (a) Zn, (b) Cu and (c) TUR removal.

that achieving optimal pollutant removal through coagulation-flocculation is notably enhanced under either alkaline or acidic conditions. This observation underscores the presence of distinct mechanisms operating in this process, emphasizing the importance of pH in maximizing the effectiveness of coagulation-flocculation for water treatment.

The majority of the studies reviewed lacked an experimental design in their methodology. Nevertheless, the incorporation of an experimental design offers several advantages, including the optimization of process parameters, prevention of experimental errors, and the determination of optimal conditions. This systematic approach allows for the maximization of efficiency and profitability in the process. When comparing these outcomes with findings from other studies, it becomes evident that the use of WMR proves highly effective and competitive with established natural coagulants. The application of an experimental design not only enhances the reliability of results but also positions WMR as a promising and robust solution in comparison to existing alternatives.

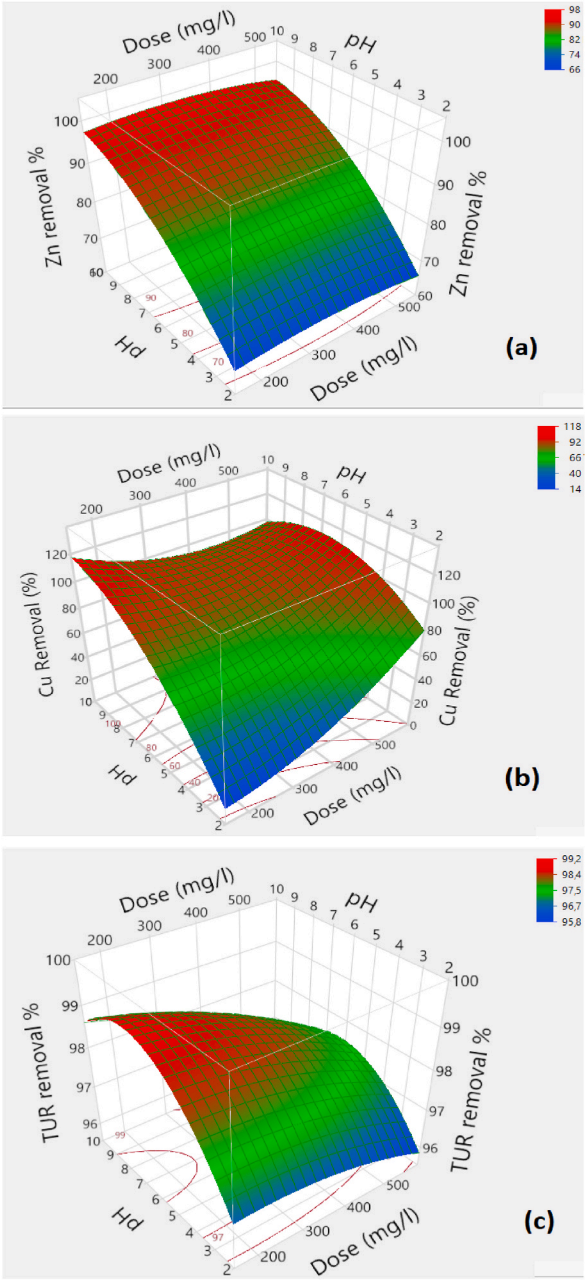

Fig. 6. Three-dimensional plot of the response surface of (a) Zn, (b) Cu and (c) TUR removal.

4. Reuse of WMR

The durability of the process of coagulation-flocculation in wastewater treatment largely depends on the recycling of coagulants [57]. Exploring methods to enhance the effectiveness of coagulant utilization is an essential environmentally-friendly strategies. This involves not only to reduce the environmental impact by reducing waste, but also to optimize the application of coagulants to achieve the desired results in terms of water treatment or purification with minimum consumption of resources [58]. The reuse of WMR is based on a simple recovery process involves filtering and then drying the sludge at 105 °C, enabling it to be reused under optimum conditions. This approach is in line with the concepts of green chemistry and environmental responsibility, by avoiding the use of additional chemicals. To assess its effectiveness, coagulation experiments were carried out over five cycles. The findings indicate that WMR can effectively achieve substantial removal rates, with Zn at 80.04 %, Cu at 81.31 %, and TUR at 86.24 %. A visual representation, as shown in Fig. 11 indicates that WMR retained its coagulation efficiency even after five cycles of reuse, with only minimal reductions, which are probably attributable to minor losses during the drying and recovery stages. Therefore, the effective and

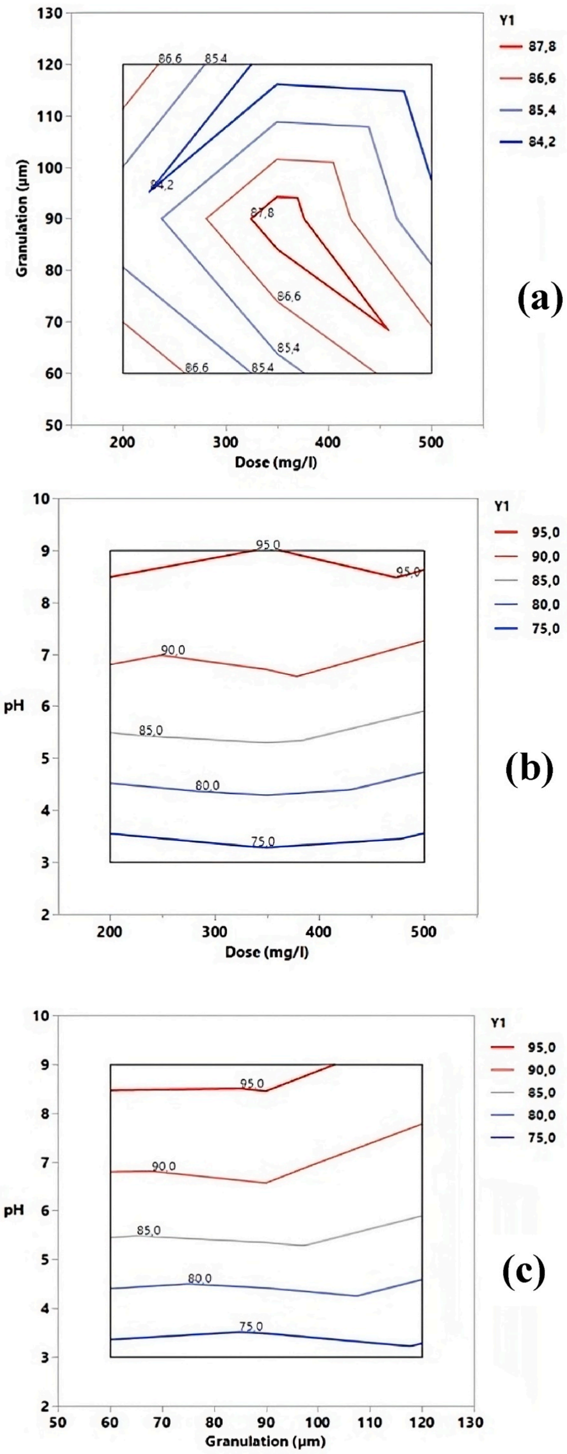

Fig. 7. Interaction between: (a) dose-granulation, (b) dose-initial pH and (c) granulation-initial pH in Zn removal.

strategic reuse of WMR is of utmost importance to ensure a sustainable coagulation-flocculation process in wastewater treatment. However, it is crucial to acknowledge that the observed decline in performance can be linked to various factors and requires a more detailed study.

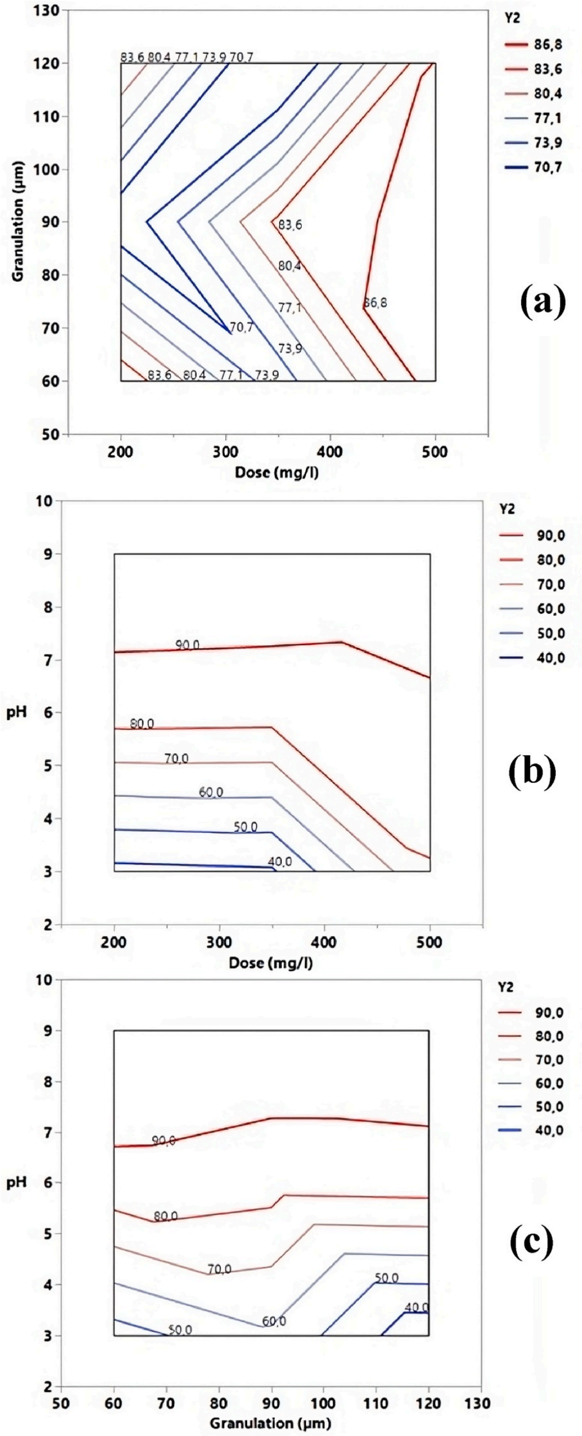

Fig. 8. Interaction between: (a) dose-granulation, (b) dose-initial pH and (c) granulation-initial pH in Cu removal.

5. Conclusion

This study systematically evaluated the effectiveness of WMR in removing Zn, Cu and TUR, using an experimental design with dose, size and pH as key variables. Utilizing the BBD, these variables were manipulated at three levels, and the experimental outcomes were found to align closely with the predicted results, as affirmed by statistical analyses. The ANOVA results further underscored the significance ($P < 0.05$) of the quadratic response patterns at a 95 % confidence level.

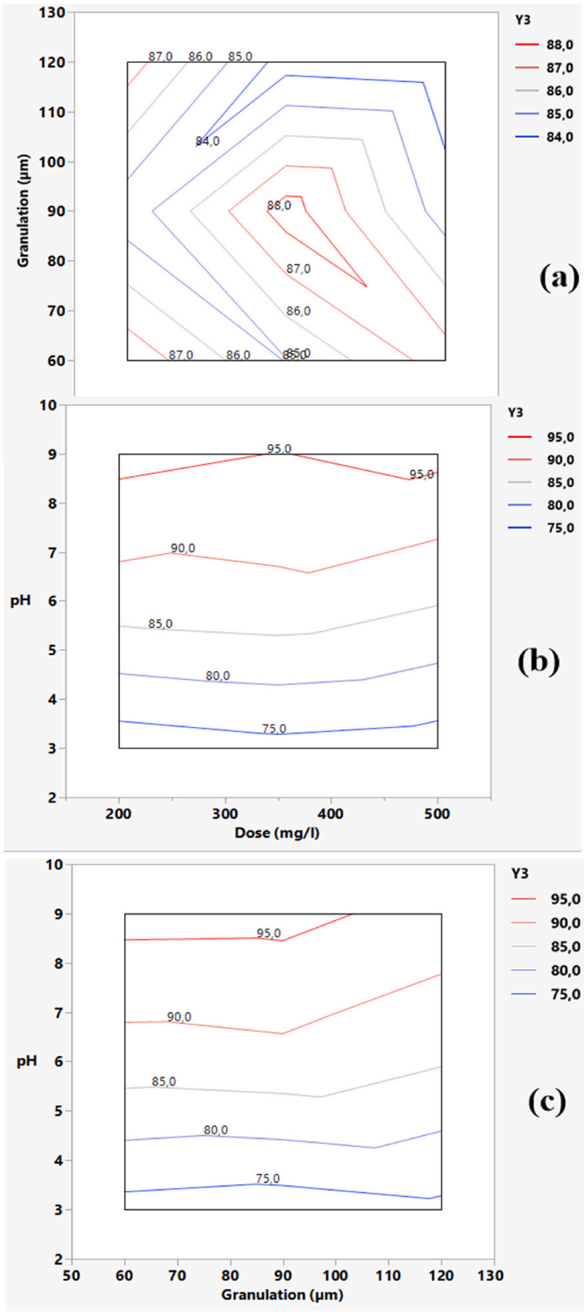

Fig. 9. Interaction between: (a) dose-granulation, (b) dose-initial pH and (c) granulation-initial pH in TUR removal.

Table 6
Comparative analysis of predicted and experimental data under optimal conditions.

Response	Optimized condition			Removal (%)		Error
	X_1	X_2	X_3	Predicted	Experiment	
Zn removal	399	60	9	98.07	97.51	0.56
Cu removal	200	90	9	100	99.88	0.12
TUR removal	200	100	7	100	99.21	0.79

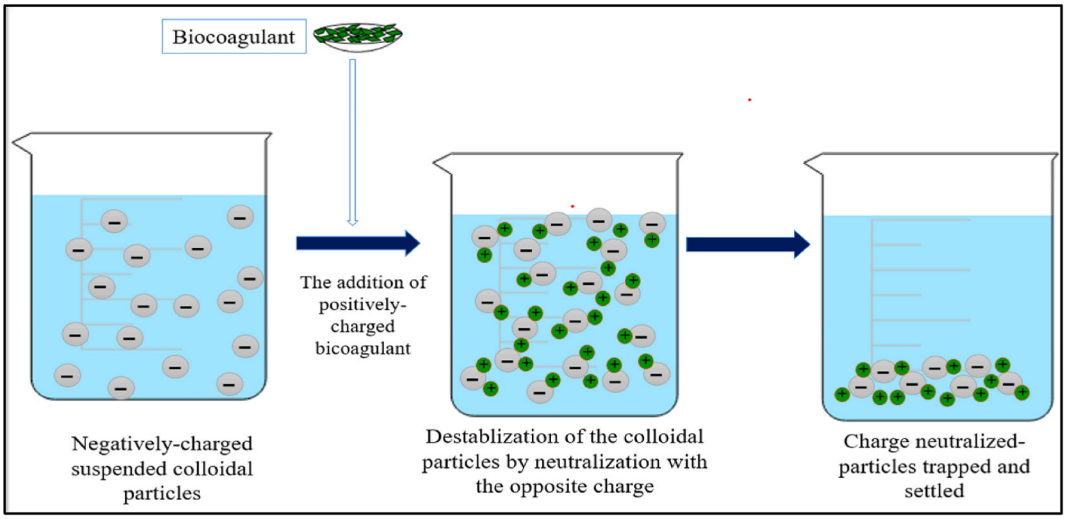

Fig. 10. Suggested mechanism during the coagulation-flocculation process.

Table 7
Comparison of some bio-coagulants for metals and turbidity removal.

Materials	Experimental design	Pollutant	Dose	pH	Efficiency (%)	Reference
Fenugreek	Central Composite Design	TUR	24.13 g/L	4.22	88.19 %	[54]
Chitosan	–	Zn	100 mg/L	4	87.9 %	[55]
Cactus	–	TUR	1.3 mg/L	10	96 %	[56]
		Cu			91 %	
		Zn			91 %	
WMR	BBD-RSM	Zn	399 mg/L	9	97.51 %	**This work**
		Cu	200 mg/L	9	99.88 %	
		TUR	200 mg/L	7	99.21 %	

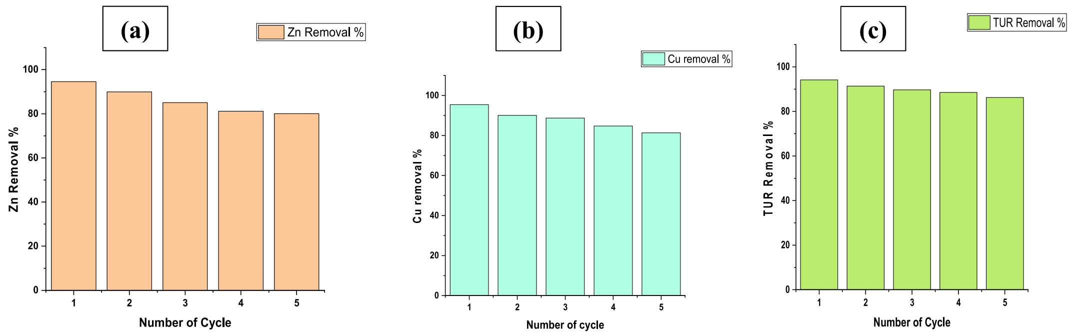

Fig. 11. Efficiency of coagulation for (a) Zn, (b) Cu, and (c) TUR removal using recycled WMR.

Optimal conditions for achieving maximum removal efficiency were determined to be: for Zn removal X_1: 399 mg, X_2: 60 μm, X_3: 9; for Cu removal X_1: 200 mg, X_2: 90 μm, X_3: 9; and for TUR removal X_1: 200 mg, X_2: 100 μm, X_3: 7. At these optimal settings, the study demonstrated exceptional removal efficiencies, reaching a maximum of 97.51 % for Zn, 99.88 % for Cu and 99.21 % for TUR, highlighting the robustness and proficiency of WMR in eliminating these contaminants.

These quantified results not only emphasize the effectiveness of WMR but also provide valuable insights into the specific operating conditions that yield optimal removal outcomes. Overall, the study contributes significantly to the understanding of the potential applications of WMR in water treatment processes for Zn, Cu, and TUR removal, paving the way for further advancements in sustainable and efficient water purification technologies.

The future perspectives of our research involve a detailed exploration of the coagulation-flocculation process by studying the influence of additional factors through experimental design tools such as stirring speed and initial concentration. This approach seeks to optimize the efficiency and effectiveness of the treatment technique. Additionally, we propose investigating the recovery of sludge generated during the treatment process, aiming for a sustainable and environmentally friendly approach. Furthermore, our study advocates for the extension of research to encompass a broader range of pollutants, including diverse dyes and metals. This expansion will contribute to a more comprehensive understanding of the applicability of our proposed method in addressing a wider spectrum of environmental pollution challenges.

Funding

This research received no external funding.

Data availability

All data generated or analysed during this study are included in this published article.

CRediT authorship contribution statement

Salma Kouniba: Writing – original draft, Data curation. **Asmaa Benbiyi:** Writing – review & editing, Validation, Supervision, Project administration. **Ali Zourif:** Software, Data curation. **Mohamed EL Guendouzi:** Validation, Supervision, Project administration.

Declaration of competing interest

The authors declare that they have no known competing financial interests or personal relationships that could have appeared to influence the work reported in this paper.

Acknowledgments

Authors would like to thank the National Center for Scientific and Technical Research (CNRST) of Morocco for putting at their disposal the technical facilities of the UATRS Division.

References

[1] A. Kali, A. Amar, I. Loulidi, C. Hadey, M. Jabri, A.A. Alrashdi, H. Lgaz, M. Sadoq, A. El-Kordy, F. Boukhlifi, Efficient adsorption removal of an anionic azo dye by lignocellulosic waste material and sludge recycling into combustible briquettes, Colloids and Interfaces 6 (2) (2022) 22, https://doi.org/10.3390/colloids6020022.

[2] A.S. Abdulkareem, W.A. Hamzat, J.O. Tijani, T.C. Egbosiuba, S. Mustapha, O.K. Abubakre, A.K. Babayemi, Isotherm, kinetics, thermodynamics and mechanism of metal ions adsorption from electroplating wastewater using treated and functionalized carbon nanotubes, J. Environ. Chem. Eng. 11 (1) (2023) 109180, https://doi.org/10.1016/j.jece.2022.109180.

[3] D. Ayodhya, Recent progress on detection of bivalent, trivalent, and hexavalent toxic heavy metal ions in water using metallic nanoparticles: a review, Results, Chem 5 (2023) 100874, https://doi.org/10.1016/j.rechem.2023.100874.

[4] Z. Fu, F. Wu, L. Chen, B. Xu, C. Feng, Y. Bai, H. Liao, S. Sun, J.P. Giesy, W. Guo, Copper and zinc, but not other priority toxic metals, pose risks to native aquatic species in a large urban lake in Eastern China, Envir, Pol 219 (2016) 1069–1076, https://doi.org/10.1016/j.envpol.2016.09.007.

[5] M. Valko, H. Morris, M.T.D. Cronin, Metals, toxicity and oxidative stress, Curr, Med. Chem. 12 (2005) 1161–1208, https://doi.org/10.2174/0929867053764635.

[6] G.S. Plumlee, T.L. Ziegler, The medical geochemistry of dust, soils and other earth materials, in: B.S. Lollar (Ed.), Environ. Geochem., 2003, pp. 264–310.

[7] P. Bjerregaard, C.B. Andersen, O. Andersen, Ecotoxicology of metals—sources, transport, and effects on the ecosystem, Handb. Toxicol. Met. (2015) 425–459, https://doi.org/10.1016/B978-0-444.

[8] M.A. Zyadah, T.E. Abdel-Baky, Toxicity and bioaccumulation of copper, zinc, and cadmium in some aquatic organisms, Bull. Environ. Contam. Toxicol. 64 (2000) 740–747, https://doi.org/10.1007/s001280000066.

[9] S. Aliyu, A.S. Ambali, T.J. Oladejo, S. Mustapha, T.C. Egbosiuba, S.O. Bada, Development of Ag-doped on multi-walled carbon nanotubes for the treatment of fish pond effluent, Reg. Stud. Mar. Sci. 58 (2023) 102797, https://doi.org/10.1016/j.rsma.2022.102797.

[10] C.F. Carolin, P.S. Kumar, A. Saravanan, G.J. Joshiba, Mu Naushad, Efficient techniques for the removal of toxic heavy metals from aquatic environment: a review, J. Environ. Chem. Eng. 5 (2017) 2782–2799, https://doi.org/10.1016/j.jece.2017.05.029.

[11] C. Qu, D. Liang, Novel electrochemical advanced oxidation processes with H_2O_2 generation cathode for water treatment: a review, J. Environ. Chem. Eng. 10 (2022) 107896, https://doi.org/10.1016/j.jece.2022.107896.

[12] M. Khalil, Y. Liu, Greywater biodegradability and biological treatment technologies: a critical review, Int. Biodeterior. Biodegrad. 161 (2021) 105211, https://doi.org/10.1016/j.ibiod.2021.105211.

[13] B.C. Hodges, E.L. Cates, J.-H. Kim, Challenges and prospects of advanced oxidation water treatment processes using catalytic nanomaterials, Nat. Nanotechnol. 13 (2018) 642–650, https://doi.org/10.1038/s41565-018-0216-x.

[14] C.A. Uko, J.O. Tijani, S.A. Abdulkareem, S. Mustapha, T.C. Egbosiuba, E. Muzenda, Adsorptive properties of MgO/WO_3 nanoadsorbent for selected heavy metals removal from indigenous dyeing wastewater. Process, Saf. Prog. 162 (2022) 775–794, https://doi.org/10.1016/j.psep.2022.04.057.

[15] C. Zhao, J. Zhou, Y. Yan, L. Yang, G. Xing, H. Li, P. Wu, M. Wang, H. Zheng, Application of coagulation/flocculation in oily wastewater treatment: a review, Sci. Total Environ. 765 (2021) 142795, https://doi.org/10.1016/j.scitotenv.2020.142795.

[16] C.S. Lee, J. Robinson, M.F. Chong, A review on application of flocculants in wastewater treatment, Process Saf. Environ. Protect. 92 (2014) 489–508, https://doi.org/10.1016/j.psep.2014.04.010.

[17] A. Benbiyi, M. EL Guendouzi, S. Kouniba, A. Zourif, Response surface modeling for malachite green removal using the box-behnken experimental design, Environ. Ecol. Res. 10 (2022) 830–838, https://doi.org/10.13189/eer.2022.100617.

[18] A.A. Owodunni, S. Ismail, Revolutionary technique for sustainable plant-based green coagulants in industrial wastewater treatment—a review, J. Water Process Eng. 42 (2021) 102096, https://doi.org/10.1016/j.jwpe.2021.102096.

[19] N.A.N. Muhamad, N.F. Juhari, I.N. Mohamad, Efficiency of natural plant-based coagulants for water treatment, IOP Conf. Ser. Earth Environ. Sci. 616 (2020) 012075, https://doi.org/10.1088/1755-1315/616/1/012075.

[20] W.M. Desta, M.E. Bote, Wastewater treatment using a natural coagulant (Moringa oleifera seeds): optimization through response surface methodology, Heliyon 7 (11) (2021) e08451, https://doi.org/10.1016/j.heliyon.2021.e08451.
[21] N.S. Al-Khalifah, A.E. Shanavaskhan, Moringa oleifera Lam., a promising crop species for arid conditions of Saudi Arabia and Moringa peregrina (Forssk.) Fiori, a native wild species for crop improvement, Int.Symp. on Moringa 1158 (2015) 159–170, https://doi.org/10.17660/ActaHortic.2017.1158.19.
[22] M.V. Jadhav, Y.S. Mahajan, Assessment of feasibility of natural coagulants in turbidity removal and modeling of coagulation process, Desalination Water Treat. 52 (2014) 5812–5821, https://doi.org/10.1080/19443994.2013.816875.
[23] C.S. Lee, J. Robinson, M.F. Chong, A review on application of flocculants in wastewater treatment, Process Saf. Environ. Protect. 92 (2014) 489–508, https://doi.org/10.1016/j.psep.2014.04.010.
[24] N.S. Zaidi, K. Muda, L.W. Loan, M.S. Sgawi, M.A. Abdul Rahman, Potential of fruit peels in becoming natural coagulant for water treatment, Int. J. Integr. Eng. 11 (2019) 140–150, https://doi.org/10.30880/ijie.2019.11.01.017.
[25] A.A. Azamzam, M. Rafatullah, E.B. Yahya, M.I. Ahmad, J. Lalung, M. Alam, M.R. Siddiqui, Enhancing the efficiency of banana peel bio-coagulant in turbid and River Water treatment applications, Water 14 (16) (2022) 2473, https://doi.org/10.3390/w14162473.
[26] M. Akter, F.B.A. Rahman, M.Z. Abedin, S.F. Kabir, Adsorption characteristics of banana peel in the removal of dyes from textile effluent, Textiles 1 (2) (2021) 361–375, https://doi.org/10.3390/textiles1020018.
[27] K.G. Akpomie, J. Conradie, Banana peel as a biosorbent for the decontamination of water pollutants. A review, Environ. Chem. Lett. 18 (2020) 1085–1112, https://doi.org/10.1007/s10311-020-00995-x.
[28] A. Muhammad, A.R. Rashidi, A. Roslan, M.M.H. Shah Buddin, Performance study of watermelon rind as coagulants for the wastewater treatment, J. Phys. Conf. Ser. 1535 (2020), https://doi.org/10.1088/1742-6596/1535/1/012053.
[29] M.M. Maoto, D. Beswa, A.I.O. Jideani, Watermelon as a potential fruit snack, Int. J. Food Prop. 22 (2019) 355–370, https://doi.org/10.1080/10942912.2019.1584212.
[30] A. Mojtahid, Pastèque développement et diversification de la production, Agriculture du Maghreb 115 (2018) 46–53. https://issuu.com/agriculturemaghreb/docs/travaux_agri_br.
[31] G. Gusmini, T.C. Wehner, R.L. Jarret, Inheritance of egusi seed type in watermelon, J. Hered. 95 (2004) 268–270, https://doi.org/10.1093/jhered/esh031.
[32] D.Z. Husein, E. Aazam, M. Battia, Adsorption of cadmium(II) onto watermelon rind under microwave radiation and application into surface water from jeddah, Saudi arabia, Arabian J. Sci. Eng. 42 (2017) 2403–2415, https://doi.org/10.1007/s13369-016-2381-2.
[33] W.A.H. Altowayti, N. Othman, A. Al-Gheethi, N.H.B.M. Dzahir, S.M. Asharuddin, A.F. Alshalif, I.M. Nasser, H.A. Tajarudin, F.A.H. Al-Towayti, Adsorption of Zn^{2+} from synthetic wastewater using dried watermelon rind (D-WMR): an overview of nonlinear and linear regression and error analysis, Molecules 26 (2021) 6176, https://doi.org/10.3390/molecules26206176.
[34] H. Gupta, P.R. Gogate, Intensified removal of copper from waste water using activated watermelon based biosorbent in the presence of ultrasound, Ultrason. Sonochem. 30 (2016) 113–122, https://doi.org/10.1016/j.ultsonch.2015.11.016.
[35] M. Berkani, Y. Kadmi, M.K. Bouchareb, M. Bouhelassa, A. Bouzaza, Combinatıon of a Box-Behnken design technique with response surface methodology for optimization of the photocatalytic mineralization of C.I. Basic Red 46 dye from aqueous solution, Arab. J. Chem. 13 (2020) 8338–8346, https://doi.org/10.1016/j.arabjc.2020.05.013.
[36] Report, Morocco, Préservation de la qualité des ressources en eau et lutte contre la pollution, Valeurs Limites de Rejet à respecter par les déversements (Normes de pollution, M.M.E.M.E.E) 1 (2014) 1–25.
[37] R.L.L. Pambi, P. Musonge, Application of response surface methodology (RSM) in the treatment of final effluent from the sugar industry using Chitosan, Water Pollut. XIII. 1 (2016) 209–219, https://doi.org/10.2495/wp160191.
[38] N. Fiol, I. Villaescusa, Determination of sorbent point zero charge: usefulness in sorption studies, Environ. Chem. Lett. 7 (2009) 79–84, https://doi.org/10.1007/s10311-008-0139-0.
[39] A.T. Nair, A.R. Makwana, M.M. Ahammed, The use of response surface methodology for modelling and analysis of water and wastewater treatment processes: a review, Water Sci. Technol. 69 (2014) 464–478, https://doi.org/10.2166/wst.2013.733.
[40] N. Wei, Z. Zhang, D. Liu, Y. Wu, J. Wang, Q. Wang, Coagulation behavior of polyaluminum chloride: effects of pH and coagulant dosage, Chin. J. Chem. Eng. 23 (2015) 1041–1046, https://doi.org/10.1016/j.cjche.2015.02.003.
[41] H. Sun, R. Jiao, H. Xu, G. An, D. Wang, The influence of particle size and concentration combined with pH on coagulation mechanisms, J. Environ. Sci. 82 (2019) 39–46, https://doi.org/10.1016/j.jes.2019.02.021.
[42] L. Zhang, J. Mao, Q. Zhao, S. He, J. Ma, Effect of AlCl3 concentration on nanoparticle removal by coagulation, J. Environ. Sci. 38 (2015) 103–109, https://doi.org/10.1016/j.jes.2015.04.014.
[43] A. Zourif, A. Benbiyi, S. Kouniba, M. EL Guendouzi, Valorization of walnut husks as a natural coagulant for optimized water decolorization, Arab. J. Chem. 17 (2024) 105399, https://doi.org/10.1016/j.arabjc.2023.105399.
[44] A.H. Jawad, Y.S. Ngoh, K.A. Radzun, Utilization of watermelon (Citrullus lanatus) rinds as a natural low-cost biosorbent for adsorption of methylene blue: kinetic, equilibrium and thermodynamic studies, J. Taibah Univ. Sci. 12 (2018) 371–381, https://doi.org/10.1080/16583655.2018.1476206.
[45] N.A. Reddy, R. Lakshmipathy, N.C. Sarada, Application of Citrullus lanatus rind as biosorbent for removal of trivalent chromium from aqueous solution, Alex. Eng. J. 53 (2014) 969–975, https://doi.org/10.1016/j.aej.2014.07.006.
[46] A. Kumar, B. Prasad, I.M. Mishra, Process parametric study for ethene carboxylic acid removal onto powder activated carbon using Box-Behnken design, Chem. Eng. Technol. 30 (2007) 932–937, https://doi.org/10.1002/ceat.200700084.
[47] A.I. Adeogun, P.B. Bhagawati, C.B. Shivayogimath, Pollutants removals and energy consumption in electrochemical cell for pulping processes wastewater treatment: artificial neural network, response surface methodology and kinetic studies, J. Environ. Manag. 281 (2021) 111897, https://doi.org/10.1016/j.jenvman.2020.111897.
[48] S. Sharma, H. Simsek, Sugar beet industry process wastewater treatment using electrochemical methods and optimization of parameters using response surface methodology, Chemosphere 238 (2020) 124669, https://doi.org/10.1016/j.chemosphere.2019.124669.
[49] P. Arulmathi, C. Jeyaprabha, P. Sivasankar, V. Rajkumar, Treatment of textile wastewater by coagulation–flocculation process using gossypium herbaceum and polyaniline coagulants, Clean 47 (2019), https://doi.org/10.1002/clen.201800464.
[50] S. Verma, B. Prasad, I.M. Mishra, Pretreatment of petrochemical wastewater by coagulation and flocculation and the sludge characteristics, J. Hazard Mater. 178 (2010) 1055–1064, https://doi.org/10.1016/j.jhazmat.2010.02.047.
[51] L. Yu, Q.W. Tang, Y.J. Zhang, R.P. Chen, X. Liu, W.C. Qiao, X. Song, A novel Fe (III) dependent bioflocculant from Klebsiella oxytoca GS-4-08: culture conditions optimization and flocculation mechanism, Sci. Rep. 6 (1) (2016) 34980, https://doi.org/10.1038/srep34980.
[52] C. Zhao, J. Zhou, Y. Yan, L. Yang, G. Xing, H. Li, P. Wu, M. Wang, H. Zheng, Application of coagulation/flocculation in oily wastewater treatment: a review, Sci. Total Environ. 765 (2021) 142795, https://doi.org/10.1016/j.scitotenv.2020.142795.
[53] N.I. Taib, N.A. Rosli, N.I. Saharrudin, N.M. Rozi, N.A.A. Kasdiehram, N.N.T. Abu Nazri, Kinetic, equilibrium, and thermodynamic studies of untreated watermelon peels for removal of copper(II) from aqueous solution, Desalination Water Treat. 227 (2021) 289–299, https://doi.org/10.5004/dwt.2021.27299.
[54] K.S. Lim, V. Sethu, A. Selvarajoo, Natural plant materials as coagulant and flocculants for the treatment of palm oil mill effluent, Mater. Today: Proc. 48 (2022) 871–887, https://doi.org/10.1016/j.matpr.2021.02.483.
[55] N. Jaafarzadeh, N. Mengelizadeh, A. Takdastan, N. Alavi, M.H. Nejad, M. Moshayyedi, Efficiency evaluation of Zinc and Nickel removal through coagulation and flocculation process using chitosan, Jentashapir J Health Res 5 (1) (2014) 451–459.

[56] O. Bouaouine, M. Baudu, F. Khalil, H. Chtioui, H. Zaitan, Comparative study between Moroccan cactus and chemicals coagulants for textile effluent treatment, J. Mater. Environ. Sci. 8 (2017) 2687–2693.
[57] J. Garvasis, A.R. Prasad, K.O. Shamsheera, P.K. Jaseela, A. Joseph, Efficient removal of Congo red from aqueous solutions using phytogenic aluminum sulfate nano coagulant, Mater. Chem. Phys. 251 (2020) 123040, https://doi.org/10.1016/j.matchemphys.2020.123040.
[58] N. El Messaoudi, M. El Khomri, A. El Mouden, A. Bouich, A. Jada, A. Lacherai, H.M.N. IqbalSikandar, I. Mulla, V. Kumar, J.H.P.A. Pinheiro, Regeneration and reusability of non-conventional low-cost adsorbents to remove dyes from wastewaters in multiple consecutive adsorption–desorption cycles: a review, Biomass Conv. Bioref. (2022), https://doi.org/10.1007/s13399-022-03604-9.